

CO5-1 Ar-Ar Dating of Sub-milligram Extraterrestrial Materials and Evaluation of the Irradiation Conditions

R. Okazaki¹ and S. Sekimoto²

¹*Department of Earth and Planetary Sciences, Kyushu University*

²*KURNS, Kyoto University*

INTRODUCTION:

Radiometric dating using a combination of K and Ar is useful for rock minerals. In the Ar-Ar dating method concentrations of the parent and daughter nuclides are determined simultaneously as $^{39}\text{Ar} / ^{40}\text{Ar}$ ratio, which is an advantage comparing to the K-Ar method. The parent ^{39}K is converted to ^{39}Ar via the $^{39}\text{K}(n, p)^{39}\text{Ar}$ reaction. In order to obtain precise data of the $^{39}\text{Ar}/^{40}\text{Ar}$ ratio, it is important to adjust the irradiation condition, such as irradiation duration, neutron flux and its energy. Especially for fine-grained crystalline or small particle samples, temperature attained during the irradiation should also be consideration.

In this study, we have investigated two irradiation conditions by using the hydraulic conveyor and the long-term irradiation plug, for the Ar-Ar dating of small extraterrestrial samples with sub-milligram.

EXPERIMENTS: Several tens to several hundred micron-sized rock fragments were recovered from meteorites (Agoult and HAH262 eucrites) and standard minerals (JG-1, orthoclase, sanidine, and wollastonite). Each of the sample particles was placed in a conical dimple ($\phi 1$, depth ~ 0.5 mm) of a sapphire disk ($\phi 5.5$, 1.5 mm thick), and covered with a sapphire disk ($\phi 5.5$, 0.3 mm thick). Each of the sapphire container was wrapped with pure aluminum foil. These Al-wrapped containers were stacked and sealed in the capsules for Hydro and Long-term irradiations. Condition of the Hydro irradiation was 36 hours under 1MW-operation + 7h under 5MW-operation, and that of the Long-term irradiation as 36 hours under 1MW-operation + 7h under 5MW-operation. After irradiation, the samples were moved to non-irradiated glass container with similar dimension from the sapphire one in order to reduce the radioactivity from the sapphire containers and Al foil. The irradiated samples were moved to Kyushu Univ. to measure noble gas isotopes. Isotopic ratios of Ar extracted from each sample by using stepped heating extraction method were determined with a modified MM-5400. Isotopes with mass of 35-39, and 41 were measured with an ion-counting detector, while ^{40}Ar was measured with

the ion-counting detector or a Daly detector.

RESULTS: We have measured noble gases in JG-1, and orthoclase samples irradiated by the Hydro and Long-term irradiations. The eucrite samples irradiated by Hydro irradiation were also measured.

Based on the $^{39}\text{Ar}/^{40}\text{Ar}$ ratio determined for the Hydro and Long-term orthoclase samples, we calculated the neutron flux and obtained J-values to be 0.013 and 0.0069 by using the K of 126400 ppm determined by EPMA and the K-Ar age of 461 Ma [1-2]. The J-value for the Long-term sample is about half of that for the Hydro orthoclase, which means that the bulk conversion rate from K to Ar is better for the Hydro than the Long-term. However, in the case of the Hydro irradiation there is a machine time limitation, so the Long-term irradiation is easier to use for Ar-Ar dating. In order to evaluate the difference in the neutron energy spectrum between the two irradiation conditions, we will conduct NAA for the standard minerals and a meteorite sample (Holbrook) that was already measured for NAA previously.

The two meteorite samples were plagioclase-rich fragments separated from eucrites, Agoult and HaH202. Plateau ages were observed between 900 and 1400 °C and between 1000 and 1400 °C for Agoult and HaH202, respectively. The average Ar-Ar ages are 4348 ± 64 and 4355 ± 60 Ma, respectively, by using the J-value calculated from the Hydro-orthoclase. These Ar-Ar ages matched well with Pu-Xe ages for the bulk samples of these meteorites.

No influence was observed in Ar isotopic ratios of the 600 °C fractions for the meteorites and orthoclase samples. However, by comparison between the orthoclase and JG-1 samples, there is a clear difference in the J-values. In both cases of the Hydro and Long-term irradiations, the J-values for JG-1 are lower than those for the orthoclase, which suggests loss of ^{39}Ar due to recoil during the irradiations. JG-1 is a biotite separate, which is a sheet silicate and is expected to cause recoil loss [3]. Therefore, the orthoclase standard mineral is better for our experiment for small rock samples.

REFERENCES:

- [1] Wartho J. A. *et al.*, (1999) Earth Planet. Sci. Lett. 170:141-153.
- [2] Nägler T. F. and Villa I. M. (2000) Chemical Geology 169:5-16.
- [3] Foland K. A. *et al.* (1992) Chemical Geology 102:269-276.

CO5-2 Volcanic and Tectonic History of Philippine Sea Plate (South of Japan) Revealed by $^{40}\text{Ar}/^{39}\text{Ar}$ Dating Technique

O. Ishizuka, S. Sekimoto¹, R. Okumura¹, H. Yoshinaga¹, Y. Iinuma¹, T. Fujii²

Geological Survey of Japan, AIST

¹*Institute for Integrated Radiation and Nuclear Science, Kyoto University*

²*Graduate School of Engineering, Osaka University*

INTRODUCTION: Submarine volcanic rocks are known to give ages different from their true eruption ages in some cases. This is due to the existence of excess ^{40}Ar in the rapidly quenched glass or Ar loss and K remobilization caused by reaction with seawater or hydrothermal fluids. Stepwise-heating analysis in $^{40}\text{Ar}/^{39}\text{Ar}$ dating is particularly useful for dating submarine volcanics.

The origin and characteristics of juxtaposing plates is critical for understanding the tectonic setting and requirements leading to subduction initiation. In case of Izu-Bonin-Mariana (IBM) arc in the Western Pacific, arc basement could be preserved in rear arc area of its ancient rear arc (i.e., Kyushu-Palau Ridge). International Ocean Discovery Program Expedition 351 recovered basement of the IBM arc in its rear arc area (Amami Sankaku Basin), and revealed that ocean crust of this basin was generated by seafloor spreading at the time of subduction initiation (Arculus et al., 2015; Ishizuka et al., 2018). However, origin and formation age of the rest of the Philippine Sea basins in the ancient rear arc is still unknown, and this hampers the understanding of the tectonic setting leading to the subduction initiation along the IBM arc.

Recent cruises in the Philippine Sea basins recovered basalts from ocean crust along the major tectonic lines such as the Oki-Daito Escarpment and Mindanao Fracture Zone of the West Philippine Basin. These samples were dated by $^{40}\text{Ar}/^{39}\text{Ar}$ dating method to obtain age of formation of the basins.

EXPERIMENTS: Samples were wrapped in an aluminum foil packet and the packets were piled up in a pure aluminum (99.5% Al) irradiation capsule (9 mm diameter and 30 mm long). The irradiation capsule was partitioned into 3 compartments to minimize the For the experiments described here, 5 mg of sample was analysed. Due to alteration of poorly-crystallized part of groundmass, the sample was treated at 100°C on hot plate with stirrer in 6N HCl for 30 minutes and then 6N HNO₃ for 30 minutes to remove possible alteration products (clays and carbonates) prior to irradiation. This procedure effectively separated and concentrated fresh plagioclase in groundmass and of microphenocryst. After this acid treatment, the separates were examined under binocular microscope before packed for irradiation.

RESULTS: $^{40}\text{Ar}/^{39}\text{Ar}$ dating of fresh basalt lavas returned some good results, show ages between 49 and 58 Ma (Fig.

1, 2). These ages are oldest ages from the WPB reported so far. Even though stratigraphic context of the samples are not clear, the data strongly implies that a part of the West Philippine Basin formed prior to subduction initiation along the Izu-Bonin-Mariana margin, and this further implies that West Philippine Basin spreading did not start as backarc spreading against Izu-Bonin-Mariana arc.

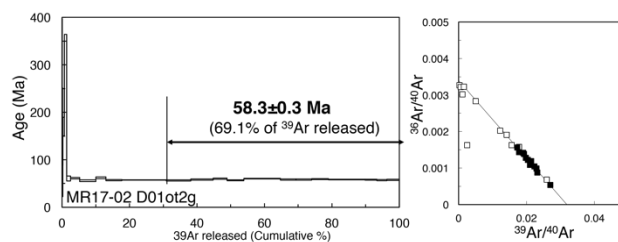


Fig. 1 Age spectrum for the basalts from the West Philippine Basin.

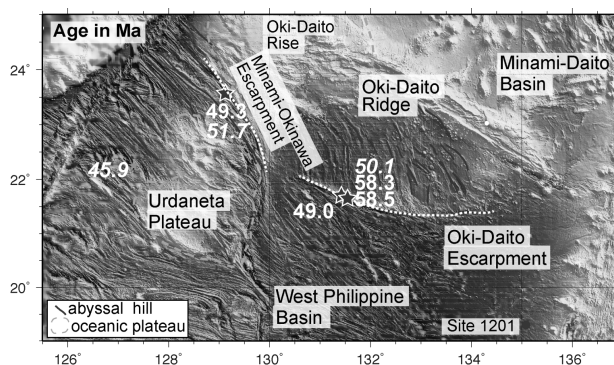


Fig. 2 Preliminary ages from the northern part of the West Philippine Basin.

REFERENCES:

[1] O. Ishizuka *et al.*, *Earth Planet. Sci. Lett.*, 481 (2018) 80-90.

CO5-3 Concentration change of soil origin elements(Al,Ca,Th) in the aerosols observed at Sakai, Osaka

N.Ito A. Mizohata, R. Okumura and Y. Iinuma
Radiation Research Center, Osaka Prefecture University,

¹ Institute for Integrated Radiation and Nuclear Science, Kyoto University

Soil aerosols which are observed mostly in coarse aerosols have various emission sources such as local or regional land surface, road dust and long distant land and desert(China continental land and dessert). Because of the different source profiles appearing the different element composition in the aerosols from these emission sources, the change in the effect from these sources would made the concentration change in the element in the aerosols that are mainly effected soil particles.

We have observed concentration of some elements, Al,Ca,Th,which might be mainly contributed from soil aerosols observed in 12 periods (P1-P12 shown in Fig.1)in 2017. Concentrations of these elements were measured by neutron activation analysis using Kyoto University Nuclear Reactor.

Samples were collected by the impactor sampler (Andersen sampler) which can obtain the aerosols by 9 particles size rages(μm), >11,7-11, 4.7-7.0,3.3-4.7,2.1-3.3,1.1-2.1,0.65-1.1,0.43-0.65,<0.43 with one week sampling period.

In this report, we have examined three elements Al, Ca, Th those might be mainly contributed from soil aerosols in coarse particle (>2.1 μm) and have different chemical behavior in the soil. Concentration change in Al,Ca and Th(Fig.1) show the period in high concentration ,P5 and P9 for Al and Ca, P5,P6 and P9 for Th, suggesting the change in effect of soil aerosol effect , P5(rich Al,Ca), P6(rich Th), P9(very rich Th).

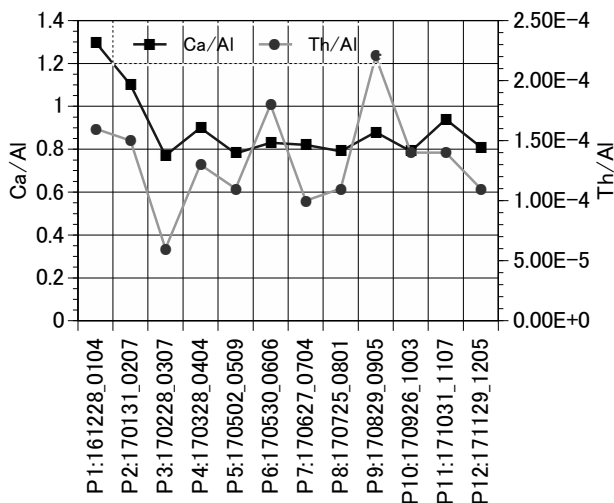


Fig.2 Change in elemental ratio based on Al concentration, Ca/Al, Th/Al.

Another indicator of emission source profile for the soil aerosols is the elemental ratio based on Al such as Ca/Al,Th/Al for which result are drawn in Fig.2. Elemental ratio based on Al (Ca/Al,Th/Al) in Fig.2 suggest some results as follows

- 1)Variation in ratio Ca/Al is smaller than that of Th/Al, showing very small variation for P3 to P12 on Ca/Al and large changing in Th/Al ($5E10^{-5}$ to $2E10^{-4}$.)
- 2) Ratio Th/Al has apparent change in P5,P6 and P9,suggesting ratio Th/Al is a good indicator for the emission source of soil particle.
- 3) Smallest ratio for Th/Al was observed in P3,in this period Kosa event is frequently observed for ordinary year , expecting Th/Al to be a good indicator for Kosa.

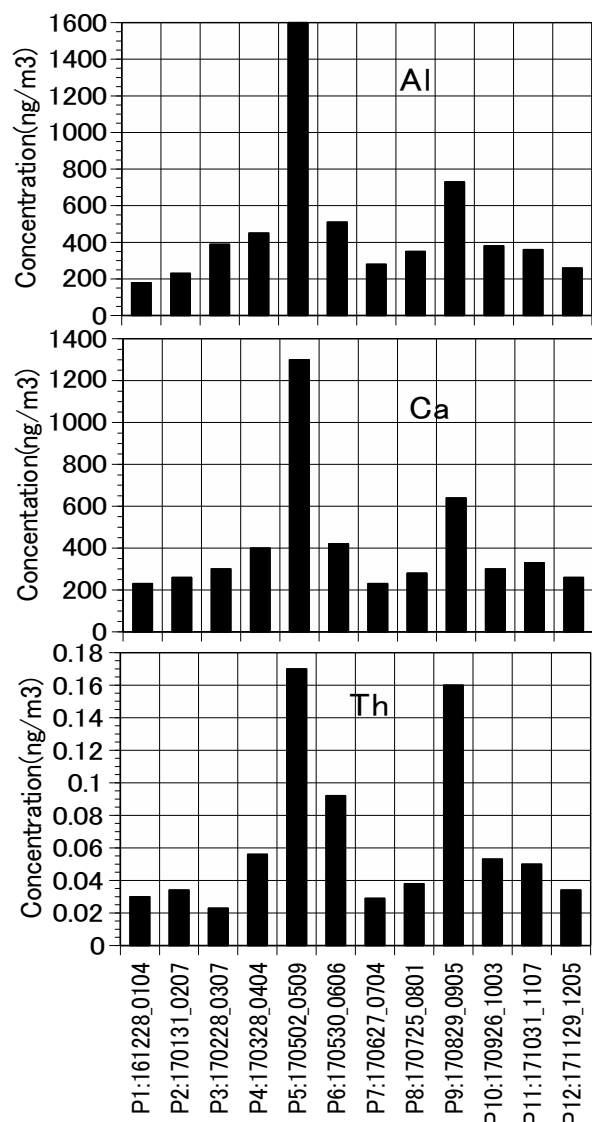


Fig.1 Concentrations of Al,Ca and Th in coarse(>2.1 μm) aerosols observed in 12 periods, 2017 at Sakai.

CO5-4 Instrumental Neutron Activation Analysis of the Steelmaking Slag, Compost and Their Mixtures in Artificial Seawater with Various Redox Conditions

M. Matsuo¹, K. Shozugawa¹, M. Yamamoto², D. Liu³, H. Iwai⁴, R. Okumura⁵, Y. Inuma⁵ and K. Takamiya⁵

¹Grad. School of Arts and Sciences, The Univ. of Tokyo

²Ocean Alliance, The Univ. of Tokyo

³National Institute of Technology, Ariake College

⁴Osaka Prefecture University

⁵Institute for Integrated Radiation and Nuclear Science, Kyoto University

INTRODUCTION: We have been conducting environmental evaluation focusing on redox sensitive elements in coastal areas. For example, Fe, Mn, Ce and Th are used because their concentration possibly increase in oxidative conditions [1]. And U is used for the evaluation of weak reductive conditions because the redox potential of U(VI)/U(IV) is between Mn(IV)/Mn(II) and S(VI)/S(-II) [2]. Recently we paid attention to serious seaweed depletions in coastal areas of barren grounds in Japan. The lack of dissolved iron is one of the possible reasons. So, we have developed a methods for restoration of seaweed beds using the mixture of steel making slag and composts [3]. The influences of redox conditions on the iron elution from the mixture were investigated by laboratorial iron elution test using artificial seawaters. In this study, as a part of above investigation, the steelmaking slag, compost and their mixtures were kept in artificial seawaters with various redox conditions and concentrations of Fe, Mn, U, Th and Ce in samples were analyzed by instrumental neutron activation analysis.

EXPERIMENTS: As test samples, steelmaking slag, compost and their mixtures were prepared. In order to get various redox conditions artificial seawaters were bubbled with oxygen, air and nitrogen. By this operation dissolved oxygen (DO) was achieved 15, 8 and 2 mg/L, respectively. Na₂S were used to achieve 0 mg/L DO. Artificial seawater was replaced every 3 days and aeration was performed. After 30 days samples were taken out and desalted by pure water washing three times and dried.

About 30 mg of samples were packed in double polyethylene film bags to perform INAA. All samples were irradiated at Kyoto University Research Reactor. Three types of gamma-ray measurement were carried out corresponding to half-lives of elements. For analysis of Mn, samples were irradiated for 10 seconds at 1 MW, and gamma-ray was measured for 600 seconds after 600 seconds. As for U, samples were irradiated for 10 minutes at 1 MW, and gamma-ray was measured for 1800 seconds after 3-6 days. As for Fe, Th and Ce, same samples as U were measured for 12000 seconds after 2-4 weeks.

RESULTS: Analysis of redox sensitive elements in samples was done by INAA method. As a result, the higher concentration of Mn was found in the samples kept in more oxidative conditions, whereas there was no significant difference in Fe. It is probably because Fe is a

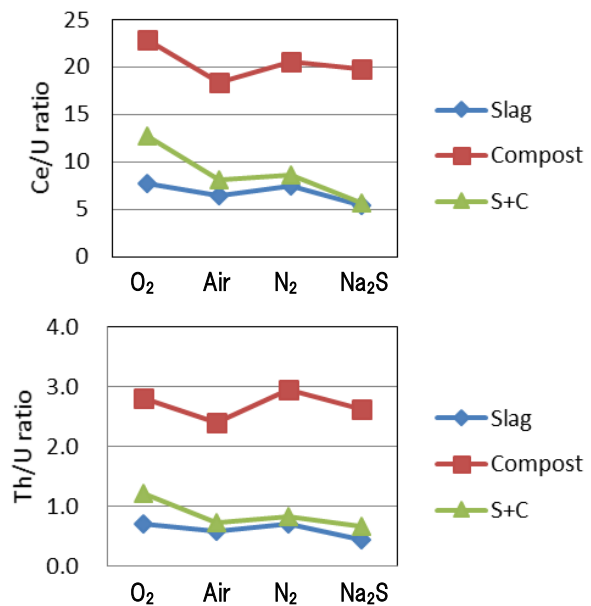


Fig. 1. Ce/U and Th/U ratios of the steelmaking slag, compost and their mixtures in various redox conditions.

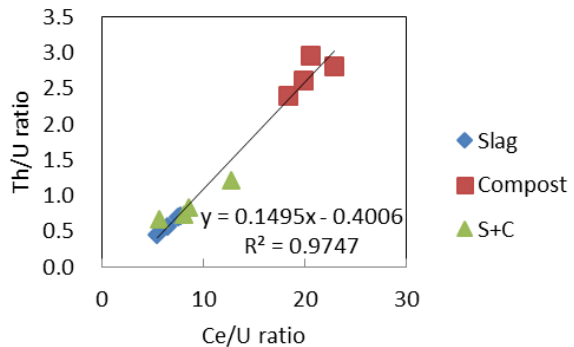


Fig. 2. Th/U-Ce/U plots of the steelmaking slag, compost and their mixtures in various redox conditions.

main element in all samples, so the small effect of change was not detected.

Ce/U and Th/U ratios for all three types of test samples were found to decrease under reductive conditions (Fig.1). In addition, we plotted the relations between Th/U and Ce/U ratios (Fig.2). The values of Th/U and Ce/U ratios at different types of samples existed on a same line. It is thought that the fact is caused by redox conditions. The chemical states of iron in same samples are also measured by ⁵⁷Fe Mössbauer spectroscopy.

REFERENCES:

- [1] D.G. Brookins, in *Eh-pH diagrams for geochemistry* (Springer-Verlag, 1988).
- [2] D.R. Turner, M. Whitfield and A.G. Dickson, *Geochim. Cosmochim. Acta*, **45** (1981), 855-881.
- [3] M. Yamamoto, M. Fukushima, E. Kiso, T. Kato, *et al.*, *J. Chem. Eng. Jpn.*, **43** (2010), 627-634.

T. Inamura, S. Fukutani¹ and K. Takamiya¹

Graduate School of Agriculture, Kyoto University

¹*Institute for Integrated Radiation and Nuclear Science,
Kyoto University*

INTRODUCTION: The concentration of Cd and As of brown rice is influenced by submerged condition of a paddy field. The submerged condition of the paddy field at the Yayoi period can be estimated from the concentration of Cd and As of the rice seed detected from the remains in the Yayoi period. However, the detected rice seed which is cultural assets must be analyzed by a non-destructive method. We have tried to analyze the concentration of Cd and As of the detected rice seed by NAA (neutron activation analysis) using pneumatic irradiation system and normal Ge-detectors, and succeeded to determine the amount of As. On the other hand, there has been found a difficulty in determination of Cd in the detected rice seeds because the seeds buried in the ground contain more mineral elements compared to fresh seeds. High concentration of mineral components such as iron and sodium would disturb the determination of other elements caused by large Compton-background observed in gamma-ray measurements. In order to decrease the Compton continuum in gamma-ray measurement to determine the amount of Cd in the rice seeds, determination of Cd has been tried by using a Ge-detector combined with Compton suppression system in the present work.

EXPERIMENTS: Buried rice seeds which weight was 1 g were double-sealed with polyethylene bags and encapsulated in a polyethylene capsule for neutron irradiation. Neutron irradiation for samples was performed using Pn-2 neutron irradiation system for 10 min and 1 hour under 5 MW operation of KUR. After the irradiation, sample stands for a few hours to decrease activities of short-lived nuclides such as ³⁸Cl, ⁵⁶Mn and ²⁴Na produced by neutron irradiation. The gamma-ray spectra of irradi-

ated samples were measured twenty times for one hour continuously by the Ge-detector combined with Compton suppression system. The detector system is composed by the Ge-detector surrounded by a well-type high-volume sodium iodine scintillation detector. The coincidental timing signals from two different detectors are processed by an anti-coincidence circuit to generate a gate signal inhibiting signals of which all energy of photon does not absorbed in the Ge-detector from registering on data acquisition system. Finally, the gamma-ray spectra of the neutron irradiated rice seeds were obtained with reduced Compton continuum and analyzed.

RESULTS: The background count rate was reduced by 30 to 70 percent at the photo peaks which energies are 93, 245 and 527 keV arisen from nuclear decay of ¹⁰⁷Cd ($t_{1/2} = 6.5$ h), ^{111m}Cd ($t_{1/2} = 48.5$ m) and ¹¹⁵Cd ($t_{1/2} = 53.5$ h) produced by neutron activation of cadmium. However, there did not found definitive photo peaks around the energies.

The amount of Cd contents in the rice seeds was assumed to be around 100 ppm producing a few tens Bq isotopes by neutron irradiation as a basis for initiation of the present experiment. But the concentration of Cd is estimated to be less than a few to a few tens ppm by detection limits of these measurement.

In order to determine cadmium of these low concentration, more irradiation time or more amount of sample is necessary. However, both the irradiation time of the Pn system is limited and the amount of sample is also limited because the sample is the detected buried rice. One possible method to determine those low concentration cadmiums is NAA using hydraulic irradiation system of KUR. The produced activities of long-lived Cd isotopes such as ¹⁰⁹Cd ($t_{1/2} = 462$ d) and ¹¹⁵Cd after one week of irradiation by the hydraulic system for maximum irradiation time are estimated as 34 and 300 Bq for 1ppm Cd in 1 g of rice seeds sample. In the near future, the higher activation by the hydraulic irradiation system will be performed to determine low concentration of cadmium in buried rice seeds sample.

CO5-6 Trace amounts of halogens (Cl, Br and I) in U.S. Geological Survey reference materials

S. Sekimoto, N. Shirai¹, M. Ebihara¹

*Institute for Integrated Radiation and Nuclear Science,
Kyoto University*

¹*Graduate School of Science, Tokyo Metropolitan University*

INTRODUCTION: Accurate and reliable data of halogen abundance have been rarely reported for terrestrial samples, as can be witnessed in the data library for geological rock samples prepared by United States Geological Survey (USGS) (at http://crustal.usgs.gov/geochemical_reference_standards/powdered_RM.html). Since halogens differ in volatility from element to element, their content and relative abundance are highly informative when discussing the petrogenesis of such samples. Recently, we have improved the radiochemical neutron activation analysis (RNAA) procedure for trace amounts of halogens (Cl, Br and I) [1]. In this study, our RNAA was applied to five reference materials that are available in USGS.

EXPERIMENTS: All the materials were in powder and were not subjected to any additional treatment such as drying. About 20-300 mg of each powder sample was weighed, inserted into a clean, small plastic vial that was sealed and then re-sealed inside a clean polyethylene bag. Chemical standard solutions of the three halogens of interest were prepared for use in the quantification by RNAA. An appropriate amount of each halogen solution (containing 90 µg of chlorine, 50 µg of bromine, and 10 µg of iodine) was dropped onto a paper disk (17 mm diameter), weighed, dried under a heat lamp and doubly sealed into polyethylene bags. Extreme care was taken when preparing the iodine reference sample.

Two USGS materials, together with a set of three reference halogen samples, were irradiated for 10 min with a thermal neutron flux of $3.3 \times 10^{12} \text{ cm}^{-2} \text{ s}^{-1}$ at Kyoto University Research Reactor Institute (KURRI)

Table 1: Cl, Br and I contents in USGS materials analyzed by RNAA in this study

(^aNot reported. ^bNumber of analysis was two.)

| sample | N | Cl (mg kg ⁻¹) | Br (mg kg ⁻¹) | I (mg kg ⁻¹) |
|--------|---|---------------------------|----------------------------|--------------------------|
| DTS-2b | 3 | 10.7 ± 0.3 | 0.093 ± 0.002 | 0.789 ± 0.148 |
| COQ-1 | 2 | 27.5 ± 1.1 | 0.071 ± 0.006 | 0.331 ± 0.094 |
| CLB-1 | 4 | 1190 ± 150 | 52.1 ± 6.8 | 599 ± 52 |
| SBC-1 | 3 | 24.9 ± 2.4 ^b | 0.355 ± 0.005 ^b | 5.07 ± 0.19 ^b |
| DGPM-1 | 2 | 315 ± 12 | 0.843 ± 0.033 | 3.55 ± 0.13 |

When a high flux reactor is used, samples need to be cooled to prevent iodine loss, however no such cooling was required with the neutron flux used in this study. After irradiation, the USGS materials were held for a few minutes to enable the decay of ²⁸Al, and were then subjected to radiochemical separation of neutron-activated halogen radionuclides (³⁸Cl, ⁸²Br, and ¹²⁸I).

The procedure of radiochemical purification for halogens, gamma-ray measurement and yield determination was essentially the same as that described in our previous work [1-2].

For the determination of iodine and chlorine, the radioactivity of ¹²⁸I and ³⁸Cl was measured by using a Ge detector for 300–1,000 s and 500–1,000 s, respectively. For bromine, ⁸²Br was measured for 50,000–100,000 s on the following few days after the radiochemical procedure. The three halogen reference samples were measured individually after the completion of the measurements, for 200-500 s for Cl and I, and 1,000–2,000 s for Br.

Chemical yields of the three halogens were determined by the reactivation method. After the completion of all gamma-ray measurements, a set of 4-6 samples (either of PdI₂ or AgBr+AgCl mixture), along with reference samples for the corresponding halogens, were irradiated for 10 sec at the same irradiation facility as used earlier. The radioactivity of ³⁸Cl, ⁸²Br, and ¹²⁸I was measured for 100 s for each nuclide.

RESULTS: Each material was analyzed two to four times. For COQ-1 (carbonatite) and DGPM-1 (disseminated gold ore) which were analyzed twice, the two analytical values for the three halogens are in agreement within uncertainties, and mean values between those two analytical values are summarized in Table 1. An uncertainty quoted for each mean value between two analytical values is just the value calculated from two individual uncertainty values accompanied by the two analytical values. Since DTS-2b (dunite), CLB-1 (coal), and SBC-1 (marine shale) have three or four analytical values for the three halogens, mean values with one sigma of standard deviation for those ten materials are also summarized in Table 1. These five USGS materials have no literature values for halogens.

Since we have demonstrated that the RNAA procedure applied in this study is effective in determining halogens in geological rock samples [1], we envisage that our RNAA data will be reflected in any future compilation in the establishment of a database of USGS geochemical reference materials.

REFERENCES:

- [1] S. Sekimoto and M. Ebihara, *Anal. Chem.*, **85** (2013) 6336-6341.
- [2] S. Sekimoto and M. Ebihara, *Geostand, Geoanal. Res.*, **41** (2017) 213-219.

CO5-7 Application of Neutron Activation Analysis to Micro Gram Scale of Solid Samples

S. Sekimoto, N. Shirai¹, M. Ebihara¹

*Institute for Integrated Radiation and Nuclear Science,
Kyoto University*

¹ *Graduate School of Science, Tokyo Metropolitan University*

INTRODUCTION: Neutron activation analysis (NAA) has been used in various research fields, such as geo- and cosmochemistry, environmental science, biology, archeology, etc. Since instrumental NAA (INAA) is a non-destructive and multi-elemental analysis method, it is suitable for precious samples and, especially, for such specimens as those highly desired to be neither physically decomposed nor chemically dissolved. Meteorites are the best example for such samples. Chondritic meteorites (chondrites) and iron meteorites contain relatively high contents of Co and Ir compared with those in the earth crust. As Co and Ir have high sensitivity in NAA, they can be good markers for the identification of such extra-terrestrial materials. In NAA of chondrites, generally, a few tens mg of specimen is used. For such a case, a few hundred $\mu\text{g kg}^{-1}$ of Ir and a few hundred mg kg^{-1} of Co can be reliably determined. When an extremely small size (e.g., micro gram) of samples such as micrometeorites recovered on the Earth surface and tiny particles returned from extraterrestrial asteroids are to be analyzed by INAA, the conventional INAA procedure used for a few tens mg is not suitable. For such tiny samples, neutron irradiation with high neutron flux and long irradiation time (namely, high neutron dose) is required. For the irradiation with high neutron dose, polyethylene bags for holding samples are not usable because they are prone to radiation damage. Polyethylene bags are also not suitable for holding tiny grain samples. It is, therefore, very important to design an appropriate sample holder for irradiating small grain samples. In our previous study [1], we have developed the INAA procedure for analyzing a single grain of down to micro and sub-micro grams in mass, and present that the INAA procedure is applicable to such samples. In this report, detection limits in the procedure is described in detail

Table 1 Detection limits for individual elements

| | Detection limit (pg) | | Concentration range in Chondrite | Content range in Chondrite of 0.05 micro-g (pg) |
|----|-------------------------------------|---|----------------------------------|---|
| | This work 45 h irradiation (1MW) | Previous work 28 h irradiation (5MW) | | |
| Na | 20 | 1 | 1800 - 6900 mg kg^{-1} | 90 - 345 |
| Sc | 0.4 | 0.03 | 6 - 11 mg kg^{-1} | 0.30 - 0.55 |
| Cr | 40 | 4 | 2650 - 4160 mg kg^{-1} | 133 - 208 |
| Fe | 2800 | 270 | 18 - 38 % | 9100 - 19000 |
| Co | 3 | 0.4 | 480 - 1100 mg kg^{-1} | 24 - 55 |
| Ni | 340 | 110 | 1.1 - 2.6 % | 550 - 1285 |
| Zn | 150 | 12 | 18 - 315 mg kg^{-1} | 0.9 - 15.8 |
| La | 0.5 | 0.1 | 235 - 585 $\mu\text{g kg}^{-1}$ | 0.012 - 0.029 |
| Sm | 0.1 | 0.02 | 140 - 294 $\mu\text{g kg}^{-1}$ | 0.007 - 0.015 |
| Ir | 0.3 | 0.02 | 380 - 1070 $\mu\text{g kg}^{-1}$ | 0.019 - 0.054 |
| Au | 0.02 | 0.01 | 120 - 330 $\mu\text{g kg}^{-1}$ | 0.006 - 0.017 |

RESULTS: Detection limits of the 11 elements measured in this study are estimated under the present experimental condition (45 h-irradiation under 1 MW operation [1]) and listed in Table 1. A detection limit is defined as a value corresponding to three sigma of background counts at the peak area of the gamma-ray emitted by a nuclide of interest. Calculated values are listed in the table, in which data for the previous experimental runs (28 or 19 h-irradiation under 5 MW operation) also are shown for comparison. Detection limit values were obtained based on data on either or both of the samples analyzed in individual runs [1-3]. The detection limit values for this study are higher than those for the previous one by factors of 2 to 20. Detection limits are dependent on experimental conditions such as the sample size, irradiation time, neutron flux, gamma-ray counting time and counting efficiency. In INAA, the detection limit is also largely controlled by the co-existing elements in the matrix. Therefore, detection limit values are to be regarded as information values but the values in Table 1 must be informative in the analysis of similar samples to those analyzed in this study, for example, micro meteorites, meteorite pieces and cosmic spherules. To evaluate the applicability of the INAA procedure described in this study, the deduced detection limits are compared with the estimated elemental contents in 0.05 μg of chondritic meteorites in Table 1. It is obvious that Na, Cr, Fe, Co and Ni can be easily determined for 0.05 μg of chondrite by INAA with 45 h irradiation under 1MW operation (this work), while INAA with more than 28 h irradiation under 5MW operation is required to determine Sc, Zn, Ir and Au. Even with the highest neutron dose (53 h irradiation under 5 MW operation) available at KUR, La and Sm may not be determined for such a small sample.

REFERENCES:

- [1] S. Sekimoto *et al.*, J Radioanal Nucl Chem, **307** (2016) 1757-1764.
- [2] M. Ebihara *et al.*, Science, **333** (2011) 1119-1121.
- [3] M. Ebihara *et al.*, Meteoritics & Planetary Science, **50** (2015) 243-254

CO5-8 Determination of Abundance of Rare Metal Elements in Seafloor Hydrothermal Ore Deposits by INAA Techniques-5: Evaluation of analytical accuracy

J. Ishibashi, Y. Tada¹, Y. Sekiya¹, S. Kawaguchi¹, K. Yonezu¹, R. Okumura², Y. Iinuma² and K. Takamiya²

Department of Earth and Planetary Sciences, Faculty of Science, Kyushu University

¹*Department of Earth Resources Engineering, Faculty of Engineering, Kyushu University*

²*Institute for Integrated Radiation and Nuclear Science, Kyoto University*

INTRODUCTION: To meet recent increased demand for rare metal elements as mineral resources, high sensitive multi-element analysis becomes more important as geochemical tools for mineral exploration. Instrumental neutron activation analysis (INAA) has the advantage of non-destructive analysis, which eliminates possible failings to exclude concentrate of elements included in specific mineral poorly soluble during acid digestion. We have conducted preliminary studies using mineralized samples collected from active seafloor hydrothermal fields, with a view to confirm and extend the range of application of this technique. Here, we report evaluation for analytical accuracy of INAA techniques, using reference ore materials.

EXPERIMENTS: We conducted a series of analysis of “Certified Reference Materials” which are provided by Natural Resource Canada. Samples were irradiated at Pn-2 (thermal neutron flux = 5.5×10^{12} n/cm²/sec at 1 MW) for 4hour (Run-1) and for 25 minutes (Run-2). For each run, the gamma ray activity was measured for 15-30 minutes after adequate cooling time (~5days for Run-1 and ~1day for Run-2). Content of each nuclide was calculated by comparison of gamma ray intensities between samples and artificial standard materials which contain known amount of Mn and Na.

RESULTS: Analytical results of the Certified Reference Materials, CCU-1d, WMA-1a, CH-4, and DS-4 are listed in Table 1. Nuclides used for the determination of elemental content are listed with their energies and half-life in minutes. Content of elements is shown together with one sigma deviations for counting the peak intensity of the gamma ray spectra. The determined contents are basically agreed with the literature values (which are reported as informational values, provisional values, or certified values in the document provided by Natural Resource Canada).

Table 1 Analytical results of “Certified Reference Materials” provided by Natural Resources Canada. Content of elements is shown with one sigma deviation for counting the peak intensity. The digits expressed in blankets are certified values reported for the Reference Materials.

| Element (unit) | Na (ppm) | As (ppm) | La (ppm) | Au (ppm) | Sb (ppm) |
|-----------------|---|----------|----------|-----------|----------|
| Nuclide | Na-24 | As-76 | La-140 | Au-198 | Sb-122 |
| energy (kev) | 2733 | 559/657 | 1596 | 412 | 564/692 |
| half-life (day) | 0.610 | 1.095 | 1.677 | 2.693 | 2.7 |
| CCU-1d | [200] | [545] | [3] | [14.01] | [61.9] |
| Run-1 | 45.6±6.6 | 230±22 | 1.3±0.1 | 52.0±0.2 | 102±12 |
| Run-2 | 93.8±4.6 | 534±53 | N.D. | 9.8±0.8 | 88±13 |
| WMS-1a | [329] | [30.9] | [4.3] | [0.300] | [6.92] |
| Run-1 | 92±10 | 20.9±2.0 | 1.0±0.1 | 0.55±0.04 | 5.3±0.6 |
| Run-2 | 216±3 | 37.6±5.9 | N.D. | 0.39±0.12 | 13.2±1.7 |
| DS-1 | [400] | [6960] | [20] | [32.59] | [107] |
| Run-1 | 75.5±8.5 | 5435±48 | 6.8±0.3 | 44.3±0.2 | 124±12 |
| Run-2 | 139±2 | 4298±23 | 0.5±0.1 | 30.8±0.2 | 274±5 |
| CH-4 | [32600] | [8.8] | [16] | [0.88] | [0.77] |
| Run-1 | 1035±98 | N.D. | 5.6±0.4 | 0.46±0.04 | N.D. |
| Run-2 | not cooled down enough because of high Na content in the sample | | | | |

N.D. means too small peak intensity of the gamma ray spectrum.

CO5-9 Siderophile element fractionation in impact glass from the Wabar impact crater

N. Shirai¹, S. Sekimoto², M. Ebihara³

¹Department of Chemistry, Tokyo Metropolitan University

²Institute for Integrated Radiation and Nuclear Science, Kyoto University

³Department of Earth Sciences, Waseda University

INTRODUCTION: Siderophile elements such as Co, Ni and PGE are depleted in crustal materials because these elements are strongly partitioned into core. In contrast, these element abundances of extraterrestrial materials such as chondrites and iron meteorites are several orders of magnitude higher than those for crustal materials. Therefore, the elevated siderophile element abundances in impact-related rock samples are due to the incorporation of meteoritic components into crustal materials. Individual chondrites and iron meteorites have characteristic absolute and relative abundances of siderophile elements. Thus, siderophile elements have been used for the detection and identification of projectile materials [e.g., 1]. Recent studies indicated that there is a possibility of elemental fractionation during impact events [e.g., 2-4]. However, processes of elemental fractionation and interaction between projectile and target materials during impact events are poorly understood. Thus, elemental fractionation leads to a difficulty in identifying projectile materials. Both projectiles and impact-related materials were collected from small and young craters such as Kamil Crater of Egypt [5] and Wabar crater of Saudi Arabia [6]. In this study, elemental abundances of impact glass from Wabar crater were determined by using instrumental neutron activation analysis (INAA) and instrumental photon activation analysis (IPAA) in order to constrain the processes of elemental fractionation during impact event.

EXPERIMENTS: Impact glass from Wabar crater was received from National Institute of Polar Research and roughly ground into small pieces. Black and white melts were separated by using tweezers and analyzed by using INAA and IPAA. INAA and IPAA were performed at Institute for Integrated Radiation and Nuclear Science, Kyoto University for the determination of elemental abundances of impact glass. For INAA, sample was irradiated for 10 sec and 4 hrs at the pn-3 and pn-2, respectively. For IPAA, the irradiation was carried out using the linear accelerator operated at 20 MeV electron beam energy and 102 μ A current for 36 hrs.

RESULTS: Our analytical results of black and white melts are consistent with the previous studies [2,6,7]. As observed by [7], black melt has higher abundances of Co, Ni, Ir and Au than those of white melt. Black melt contains 300 ppm for Co, 3710 ppm for Ni, 336 ppb for Ir and 5.72 ppb for Au. Mass fractions of Wabar iron in the black melt analyzed in this study were estimated to be 4 to 6% based on Co, Ni and Ir abundances for Wabar iron [2] and black melt [this study]. Assuming that target ma-

terial has similar siderophile element abundances to those of upper continental crust, impact-related material having 4 to 6% mass fraction of projectile has similar chemical characteristics of siderophile elements. Figure compares siderophile elements abundances of black melt with those of bulk Wabar iron. Siderophile element abundances were normalized to Ni and those for bulk Wabar iron. Black melt has higher Co/Ni ratio and lower Ir/Ni and Au/Ni ratios compared with those of bulk Wabar iron. For comparison, siderophile element abundances of kamacite and taenite from Wabar iron are shown in Fig. Ir/Ni ratio of black melt falls in the range between those of kamacite and taenite. However, Au in black melt are highly depleted compared with kamacite and taenite. Based on our analytical results of INAA and IPAA, projectile could not be simply incorporated into target material.

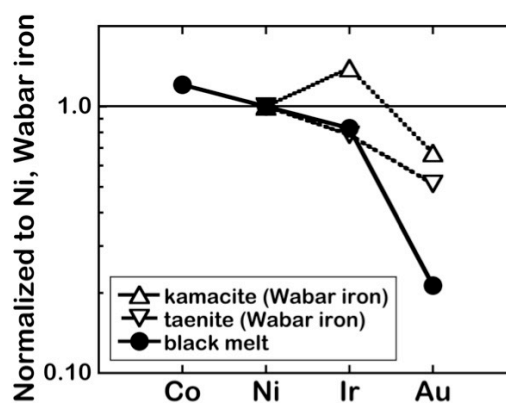


Fig. Siderophile elements of black melt (this work) and kamacite and taenite from Wabar iron (Mullane et al. [8]).

REFERENCES:

- [1] R. Tagle and J. Berlin Meteorit. Planet Sci., **43** (2008) 541-559.
- [2] D. W. Mittlefehldt *et al.*, Meteoritics, **27** (1992) 361-370.
- [3] S. Jonášová *et al.*, Geochim. Cosmochim. Acta, **190** (2016) 239-264.
- [4] S. Goderis *et al.*, Geochim. Cosmochim. Acta, **217** (2017) 28-50.
- [5] A. Fazio *et al.*, Meteorit. Planet Sci., **49** (2014) 2175-2200.
- [6] E. Gnos *et al.*, Meteorit. Planet Sci., **48** (2013) 2000-2014.
- [7] F. Hörz *et al.*, Proc. Lunar Planet. Sci Conf., **19th** (1989) 697-709.
- [8] E. Mullane *et al.*, Chem. Geol., **208** (2004) 5-28.

CO5-10 Change of uptake of radioactive cesium from contaminated soil to rice plants

M. Yanaga, Y. Dezawa¹, H. Yoshinaga², R. Okumura² and Y. Iinuma²

Center for Radioscience Education and Research,
Faculty of Science, Shizuoka University

¹Department of Science, Graduate School of Integrated
Science and Technology, Shizuoka University

²KURNS, Kyoto University

INTRODUCTION: A large quantity of radioisotopes, such as ¹³¹I, ¹³⁴Cs, ¹³⁷Cs, ¹⁴⁰Ba and ¹⁴⁰La, were released in to the atmosphere by the Fukushima Daiichi Nuclear Power Plant accident and contaminated the air and ground [1-3]. Radioactive cesium is especially a problem because of its long half-life (30 years for ¹³⁷Cs) among the released radioisotopes. Paddy field soil was also contaminated with radioactive cesium. Separating radioactive cesium from the soil is necessary to prevent damage by rumors although there have been no reports that activity of rice produced in Fukushima prefecture exceeding the reference value was detected in recently.

However, simple removal of contaminated soil would create a vast quantity of radioactive waste. Recently, we found that the absorption of radioactive cesium from artificially contaminated soil into rice plants increased by adding a stable isotope to irrigation water. In this study, cultivation experiments in laboratory were conducted by using paddy field soil collected in Fukushima city to examine whether rice grow normally or not even if stable isotope of cesium is added, based on a change of the trace element concentration, and also to confirm whether the absorption of radioactive cesium from really contaminated soil increase or not.

EXPERIMENTS: Materials and Method Soils contaminated with radioactive cesium were collected from paddy fields located in two areas (O area and Y area) of Fukushima city. Rice seedlings were transplanted to 9 Wagner pots (1/5000 a) filled with 2.7 kg air-dried soil of O area and to another 10 pots filled with soil of Y area. The transplanted pots for each area were divided into three groups, respectively, such as O-I, O-II and O-III; Y-I, Y-II and Y-III. Ground water in Shizuoka city was used as irrigation water through a period of cultivation. The number of pots for each group was three except for group Y-III(4 pots). After midseason drainage followed by irrigation, 2.0×10^{-3} mol and 6.0×10^{-3} mol of CsCl were added as aqueous solution into the pots of group I (O—I and Y-I) and group II (O-II and Y-II), respectively.

The rice plants were separated into brown rice, straw and leaf after harvest. They were dried and transferred to U8 containers. After measurements of radioactivities of ¹³⁷Cs and ¹³⁴Cs in them, 50 - 60 mg of each sample were doubly wrapped in a polyethylene film and subjected to INAA.

INAA The samples in polyethylene capsules were irradiated in Pn-3 for 90 seconds and in Pn-2 for 4 hours, for short and long irradiation, respectively. As comparative standards, the certified NIST Standard Reference Material 1577b Bovine Liver as well as elemental standard for Cs was used. The γ -ray spectroscopic measurements with an HPGe detector were performed repeatedly for the short-irradiated samples: the first measurements for 120 - 900 seconds after decay time of 5 - 15 minutes and the second one for 250 - 1200 seconds after 60 - 150 minutes. The long-irradiated samples were measured for 1 - 24 hours after an adequate cooling time (15 - 60 days).

RESULTS: The absorption amount in groups which were added with cesium stable isotope increased compared with the groups which were not added. This indicates that addition of stable cesium isotope is effective for the removal of radioactive cesium from soil. However, as shown in Fig. 1, addition of large amount of stable cesium caused an obstacle to growth of rice plant. INAA results showed that the concentrations of Mn in leaf and straw of group O-II and Y-II were distinctly lower than the others.

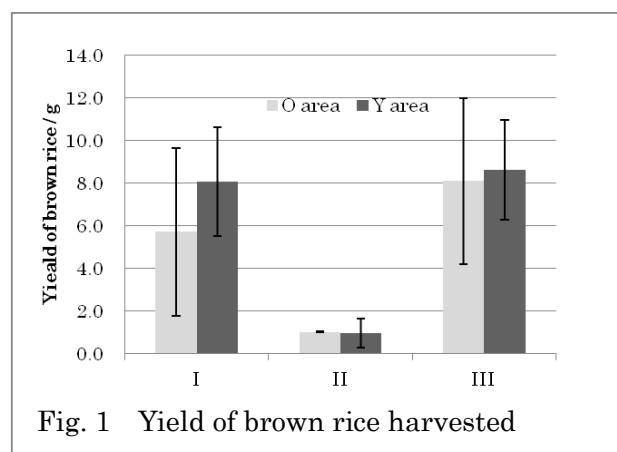


Fig. 1 Yield of brown rice harvested

REFERENCES:

- [1] S. Endo *et al.*, J. Environ. Radioact., **111** (2012)18-27.
- [2] M. Yanaga and Y. Oya, Radiation Safety Management, **12** (2013)16-21.
- [3] M. Yanaga *et al.*, Radiation Safety Management, **12** (2013)37-42.

H. Hyodo¹, K. Sato^{1,2,3}, H. Kumagai³ and K. Takamiya⁴

¹ Institute of Frontier Science and Technology,
Okayama University of Science

² Department of Applied Chemistry and Biochemistry,
National Institute of Technology, Fukushima College

³ Submarine Resources Research Center, Japan Agency
for Marine-Earth Science and Technology

⁴ Institute for Integrated Radiation and Nuclear Science,
Kyoto University

INTRODUCTION: Gneisses in the east coast of Labrador area consist a part of potential oldest crust, as they have recorded several early Archean events. The oldest zircon age reported is 3.9 Ga [1] in the area. It is of much interest to compare the thermal history with that of the Acasta area where the oldest rocks are found [2]. We have carried out ⁴⁰Ar/³⁹Ar dating on zircon grains from the Labrador area. Zircon normally does not have potassium as its component, but it often has inclusions in forms of fluid and/or minerals which may contain potassium. If zircon could behave as a solid container for its inclusions against later disturbances, the inclusions may keep the primary record when they are formed, and may provide some insights on the Precambrian environments. Variety of inclusions might behave separately, but average behavior could be determined from the experiment.

EXPERIMENTS: Experimental procedure is the same as described previously [3]. Rock samples were crushed, and sieved in #25-100 mesh. After ultrasonic cleaning in distilled water, single mineral grains were handpicked. The zircon grains were irradiated in the KUR for 22 hours at 1 MW and subsequently 6 hours at 5MW. The total neutron flux was monitored by 3gr hornblende age standard [4], which was irradiated in the same sample holder. In the same batch, CaSi₂ and KAlSi₃O₈ salts were used for interfering isotope correction. A typical J-value was $(1.183 \pm 0.009) \times 10^{-2}$. In stepwise heating experiment, temperature of a mineral grain was measured using infrared thermometer whose spatial resolution is 0.3 mm in diameter with a precision of 5 degrees. The amount of argon isotopes in inclusions seems to be small. In some cases when grain sizes are too small for the analyses, multiple (3-5) grains were heated under defocused beam in order to increase the sample size. Extracted argon isotopes were measured using a custom-made mass spectrometer [3].

RESULTS: Figure 1 illustrates one of ⁴⁰Ar/³⁹Ar age spectra of a single zircon grain. Because of the difficulty in temperature control and small amount of argon release, number of heating steps was only a few. Most zircon grains did not release much argon below 1000 degrees starting from 600 degrees. However, 3.8 Ga age was found in the first step in this case. This probably reflects the characteristics of the inclusions. Average behavior of the zircons was heat resistant.

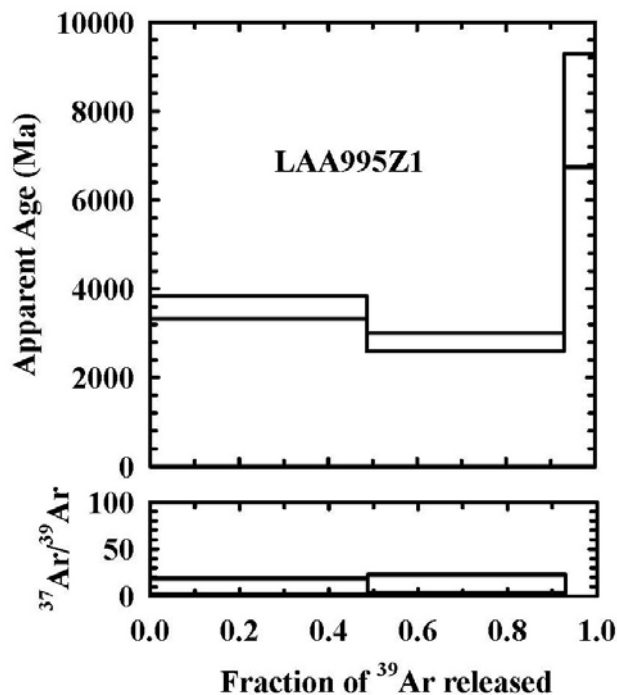


Fig. 1. ⁴⁰Ar/³⁹Ar age spectra of zircon from east coast of the Labrador area, Canada. Although the error seems to be large due to the small amount of ³⁹Ar, some apparent ages are comparable to the U-Pb zircon age.

It is difficult to define a plateau in this diagram. However, the apparent ages seem to be surprisingly old compared to the results from the Acasta gneisses [5]. The similar trend of Archean ages was also found in the results of other Labrador zircon. Presence of variety of inclusions is probably disturbing to obtain a plateau age in the zircons. In this case, the results suggest a possibility of recovering the Archean ages by ⁴⁰Ar/³⁹Ar method comparable to the U-Pb results.

REFERENCES:

- [1] T. Komiya, *et al.*, *Geoscience Frontiers* **8** (2017) 355-385.
- [2] S.A. Bowring and I.S. Williams, *Contributions to Mineralogy and Petrology*, **134** (1999) 3-16.
- [3] H. Hyodo, *Gondwana Research* **14** (2008) 609-616.
- [4] J.C. Roddick, *Geochim. Cosmochim. Acta* **47** (1983) 887-898.
- [5] H. Hyodo, K. Sato and H. Kumagai, KURRI Progress Report 2017 CO5-15.

H. Ohira, T. Kondo and Y. Sampei

Department of Earth Science, Shimane University

INTRODUCTION: Cretaceous to Paleogene granite in Oku-Izumo area is strongly weathered into granite sand. From the 16th Century to the 1900s, the “Tatara” steel manufacture, using iron sands (magnetite grains) extracted from the granite sand was operated in this area. In the process of extraction of magnetite, the landform of this area was considerably transformed by Kanna-Nagashi, in which outcrops of weathered granite was cut out and large amount of quantity of granite sand was washed in running water along gutter. The granitic basement of this area is classified into several bodies and the age of typical granite body (the Yokota granite) is measured to be 59.6 ± 5.5 Ma by Rb-Sr whole rock isochron method [1]. The age of another body (the Abire granite) which produced large amount of iron sand was also measured to be 60.5 ± 6.3 Ma [2]. These ages show the period of emplacement of granite, considering with the higher closure temperature of Rb-Sr system. However ages with lower closure temperature which enables estimation of cooling history of rocks has not been reported. Cooling and uplift history might have some kind of relationship with weathering of this area and the formation of granite sands. In this report, apatite and zircon fission track ages with relatively lower closure temperature and schematic cooling history are discussed.

EXPERIMENTS: Rock was crashed, sieved and washed to separate fractions less than 0.3mm. Heavy minerals were concentrated using conventional method of heavy liquid and magnetic separator. Apatite grains were mounted in epoxy resin, polished to reveal a complete internal surface, and etched in 7% HNO₃ solution in 20-25seconds at 25°C. Zircons were mounted in PFA Teflon, polished and etched in a NaOH-KOH eutectic melt at 225°C [3]. Samples were irradiated at pneumatic tube of graphite facility (Tc-pn) of Kyoto University Reactor (KUR). After irradiation, external detectors (mica) were etched in 46% HF at 25°C for 6-7 minutes (for mineral mounts) and for 20-50min (for NIST-SRM612 glass). FT density was measured at 1000× magnification with a dry objective.

RESULTS: Apatite and zircon ages from typical outcrops of granite sand near the Hanaidani (the ruin of “Kanna-Nagashi”) were measured to be 43.4 ± 3.4 Ma and 53.9 ± 2.8 Ma, respectively. This sampling site belongs to the Abire granite measured to be 60.5 Ma by Rb-Sr method [2]. The discrepancy of above radiometric ages is probably due to the difference of closure temperature of each dating method. Closure temperature of apatite and zircon FT and whole rock Rb-Sr method are thought to be around 100°C [4], 240°C [5] and 700°C [6]. Consid-

ering with above closure temperatures and obtained ages, the age-temperature plot (cooling history) is illustrated as shown in Fig.1. The evidence of remarkable hydrothermal alteration such as sericite veins are rarely observed in thin section of granite sand, suggesting that thermal influence for fission track system is probably negligible. The cooling curve shows relatively fast cooling rate (69.7°C/Ma) at a higher temperature range probably due to conductive cooling after emplacement of granite at a deeper depth. In contrast, the lower cooling rate (1.96°C/Ma) at a temperature range less than 100°C is presumably due to uplift and exhumation of granite of this area. Assuming a constant and normal geothermal gradient of 3°C/100m, surface temperature of 15°C and simple constant uplift, a schematic denudation rate of 6528m/Ma (0.065mm/year) is obtained. Fission track length measurement is required to discuss more detail cooling history. Fission track age of fine-grained granodiorite which sporadically distributed among the granite was additionally measured to be 26.5 ± 1.1 Ma. Thermal influence of such younger intrusion affects the cooling history of the older granite should be examined.

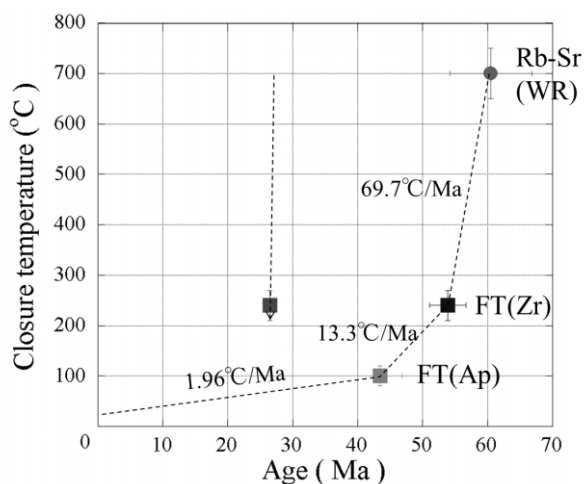


Fig. 1. Schematic cooling history of typical weathered granite collected near the Hanaidani ruin and the younger plutonism newly identified in Oku-Izumo area.

- [1] Nishida K. *et al.*, 2005, *J. Geol. Soc. Japan*, 111, 123-140. (in Japanese with English abstract)
- [2] Iwata C. *et al.*, 2013, *J. Geol. Soc. Japan*, 119, 190-204. (in Japanese with English abstract)
- [3] Gleadow A.J.W. *et al.*, 1976, *Earth and Planetary Science Letter*, 33, 273-276.
- [4] Sueoka S. *et al.*, 2016, *Geoscience Frontiers*, 7, 197-210.
- [5] Hurford. A.J., 1986, *Contrib. Mineral Petrol.*, 92, 413-427.
- [6] Yuhara *et al.*, 2013, *Earth Science (Chikyu Kagaku)*, 67, 161-168. (in Japanese with English abstract)

CO5-13 Halogen Systematics in Mantle Xenoliths from the Western Pacific Subduction Zones

H. Sumino, A. Takenouchi, M. Koike, R. Okumura¹, Y. Inuma¹ and S. Sekimoto¹

University of Tokyo

¹ *Institute for Integrated Radiation and Nuclear Science, Kyoto University*

INTRODUCTION: Volatiles, such as water, carbon dioxide, halogens, and noble gases, concentrate on the surface of the Earth, because of their high volatilities. They are continuously expelled from the interior of the Earth by volcanisms at mid-ocean ridges, hot spots, volcanic arcs. On the other hand, oceanic plates transport volatiles into the interior of the Earth via subduction processes. Through decomposition of volatile-bearing minerals such as hydrous minerals, those volatiles are released into the mantle wedge, which may result in major changes to the chemical and physical properties of mantle rocks. However, despite their importance, the detail of volatile cycling in subduction zones remains poorly constrained.

Halogens are among the most powerful tracers of volatile cycling in subduction zones. Based on elemental compositions of heavy halogens (Cl, Br, and I) in subduction zones, the importance of sedimentary pore fluid-like iodine-rich halogens transported by serpentine has been pronounced (e.g., [1,2]). Halogen compositions in mantle beneath volcanic fronts have been overwhelmed by the sedimentary pore fluid-like halogens [2]. Whereas subducted seawater- or sedimentary pore fluid-like heavy noble gases (Ar, Kr, and Xe), which are also powerful tracers of volatile cycling, significantly extend into the convecting mantle [3], mantle xenoliths from intraplate settings suggest that subducted sedimentary pore fluid-like halogens have been negligible in the convecting mantle [4]. However, there is a large missing link between volcanic fronts and the convecting mantle. In this study, we measured compositions of halogens and noble gases in mantle xenoliths from rear-arc region in the Western Pacific subduction zones.

EXPERIMENTS: The mantle xenoliths used in this study are from rear-arc regions in the Western Pacific subduction zones: the Ichinomegata volcano (the Oga peninsula, Northeast Japan), the Jeju Island (south of the Korean peninsula), the Oki-Dogo Island (Southwest Japan), the Ilchan and Sveyagin volcanic bodies in Sikhote-Alin (Far Eastern Russia), and the Takashima Island (Southwest Japan).

Halogens in the samples were analyzed using neutron irradiation noble gas mass spectrometric technique (e.g., [5]). In this method, halogens (F, Cl, Br, and I) and some elements (K, Ca, Ba, and U) are converted to corresponding isotopes of noble gases (Ar, Kr, and Xe) by neutron irradiation in a nuclear reactor. Because of relatively high cross-sections for neutron capture and high sensitivity of noble gas mass spectrometer, trace amounts

of heavy halogens (Cl, Br, and I) in mantle xenoliths, which are difficult to analyze using conventional methods in geochemistry, can be quantified.

The mantle xenolith samples were coarsely crushed into 0.5–2 mm. Neutron irradiation for the mantle xenoliths were irradiated neutron in the Kyoto University Research Reactor (KUR) for 5 hours. Thermal and fast neutron fluxes were determined by analyses of Hb3gr hornblende that was irradiated with the mantle xenoliths samples. Noble gases in the neutron-irradiated samples were analyzed using a noble gas analysis system at the University of Tokyo [5]. The samples were crushed using a hydraulic press and the remaining powder was melted in a W-coil furnace to extract noble gases.

RESULTS: The mantle xenoliths from rear-arc regions showed a wide range of I/Cl and Br/Cl ratios. All of data can be explained by mixing among sedimentary pore fluid-like high I/Cl component, high Br/Cl component, and MORB source mantle-like component. Correlation between the Cl and CaO concentrations suggests that clinopyroxenes controls halogen signatures in bulk lherzolites at least in the mantle beneath the Ichinomegata volcano. The high I/Cl and Br/Cl samples showed arc type signatures in trace element compositions, suggesting that these halogens are slab-derived halogens. These evidences indicate that multiple halogen components are present in the mantle beneath rear-arc regions and that they are not a consequence of elemental fractionation from a common source. The presence of halogens inherent in the mantle indicates that subducted halogens are not overwhelming in rear-arc regions, whereas subducted halogens are overwhelming in the mantle beneath volcanic fronts [2]. This difference in the extent of subduction influence is also observed in halogen/⁴⁰Ar* ratios, where ⁴⁰Ar* is non-atmospheric ⁴⁰Ar. The ratios decrease toward the depleted mantle values in the order of volcanic front > rear-arc region > intraplate setting, indicating that the extent of subduction influence decreases in this order. Halogen/⁴⁰Ar* ratios have an advantage that the ratios are less affected by contamination, especially that from air. This advantage and the variation of the halogen/⁴⁰Ar* ratios of mantle xenoliths from various geological settings suggest that halogen/⁴⁰Ar* ratios can be used as a reliable proxy of the extent of subduction influence.

REFERENCES:

- [1] H. Sumino *et al.*, *Earth Planet. Sci. Lett.*, **294** (2010) 163-172.
- [2] M. Kobayashi *et al.*, *Earth Planet. Sci. Lett.*, **457** (2017) 106-116.
- [3] G. Holland & C. J. Ballentine, *Nature* **441** (2006) 186-191.
- [4] M. Kobayashi *et al.*, *Geochemistry, Geophysics, Geosystems* **20** (2019) 952-973.
- [5] M. Kobayashi, Ph.D. Thesis, Univ. Tokyo (2017).

CO5-14 Neutron activation analysis for environmental materials (sediments of Lake)

Y. Okada, N. Hagura¹, H. Matsuura¹, T. Uchiyama and Y. Iinuma²

Atomic Energy Research Laboratory, Tokyo City University

¹Department of Nuclear Safety Engineering, Tokyo City University

²KURNS, Kyoto University

INTRODUCTION: Contamination of radioactive Cs of Lake Akagi Onuma Lake in Gunma Prefecture was observed due to the accident at Fukushima Daiichi Nuclear Power Station. Recently, the levels of radioactive Cs in wakasagi that live there have been slowly decreasing with the decrease of that of the lake water. In order to clarify the cause of the gradual collapse, we have been investigating the inhabiting organisms and their surrounding areas for 7 years ^{1, 2}. This study will be conducted as part of investigating the contribution of sediments to lake water.

EXPERIMENTS: Environmental materials were sediments of Lake Onuma on Mt. Akagi. Sediment samples were collected from the center of Lake Onuma (N36°33'46", E139°10'46") using a Satake-type core sampler. The core sediment samples were then cut every 2cm from the surface up to the 50cm length depth. The cut samples were dried at 105°C, pulverized in a mortar. The analysis samples were 3 samples respectively from sediments of 10 mm, 160 mm and 390 mm in depth. Those samples were prepared by doubly packing in clean poly-ethylene bags. Six samples (ca.50mg) and comparative standards (JLK1-1, NIES8) were irradiated for a short time (30s) at thermal neutron flux of 4.68×10^{12} n/cm² and for a long time (3600s) at a thermal neutron flux of 5.5×10^{12} n/cm² in KUR. For monitoring the neutron flux, about 9mg of aluminum wires containing 1.5% Sb and about 11mg Fe wires were doubly packed in clean polyethylene bags and irradiated together with the samples and comparative standards. The irradiated samples were measured by conventional γ -ray spectrometry using a coaxial Ge detector. Analysis of γ -ray spectrometry were at Gamma Station (SEIKO EG&G Co.,LTD).

RESULTS: As a result of measuring the neutron flux in the irradiation capsule, the flux ratio of the upper stage and the lower stage in the capsule was approximately 1.0. Table 1 lists the concentration of 19 elements in sediments from sediments of 10 mm, 160 mm and 390 mm in depth of Lake Onuma on Mt. Akagi. This time, only the results obtained from long-time irradiation were reported. The determined values of many elements in three samples at the same depth showed good agreement. Fig. 1 (York,1996), Vol. 1.

shows the concentrations of trace elements in sediments by depth. The elements that tend to increase in concentration with increasing depth were Lu, Eu, Yb, Ce, Sc and Co. On the contrary, the elements which tend to decrease in concentration with increasing depth were Br, Sb and Cs.

Table 1 Element concentrations in the core sediments of Lake Onuma on Mt. Akagi. Unit: $\mu\text{g/g}$

| elements | 10mm | | | | 160mm | | | | 390mm | | | |
|-----------------------|-------|-------|-------|-------|-------|-------|-------|-------|-------|-------|-------|-------|
| | 1 | 2 | 3 | Av. | 1 | 2 | 3 | Av. | 1 | 2 | 3 | Av. |
| U | 0.655 | 0.674 | 0.676 | 0.668 | 1.196 | 0.994 | 1.525 | 1.24 | ND | ND | 1.046 | 1.05 |
| Lu | 0.162 | 0.134 | 0.146 | 0.147 | 0.222 | 0.217 | 0.236 | 0.225 | 0.281 | 0.275 | 0.273 | 0.28 |
| Eu | 0.597 | 0.610 | 0.580 | 0.596 | 0.673 | 0.666 | 0.691 | 0.673 | 1.00 | 1.027 | 0.988 | 1.01 |
| Ba | 182 | 220 | 158 | 187 | 272 | 244 | 264 | 260 | 203 | 182 | 195 | 193 |
| Hf | 1.64 | 1.67 | 1.56 | 1.62 | 2.15 | 2.22 | 2.20 | 2.19 | 1.84 | 1.94 | 1.93 | 1.91 |
| Yb | 1.21 | 1.27 | 1.30 | 1.26 | 1.31 | 1.34 | 1.60 | 1.42 | 1.90 | 1.87 | 1.95 | 1.91 |
| Ce | 22.3 | 20.1 | 18.5 | 20.3 | 26.1 | 22.8 | 25.8 | 24.9 | 32.6 | 38.1 | 49.1 | 39.9 |
| Pb($\mu\text{g/g}$) | 1.23 | 1.24 | 1.33 | 1.27 | 1.26 | 1.25 | 1.51 | 1.34 | 2.86 | 3.12 | 3.22 | 3.07 |
| Pb($\mu\text{g/g}$) | 3.01 | 3.03 | 2.71 | 2.92 | 3.34 | 3.25 | 3.13 | 3.24 | 3.13 | 3.15 | 3.17 | 3.15 |
| Th | 2.39 | 2.35 | 2.22 | 2.32 | 3.31 | 3.40 | 3.54 | 3.42 | 1.75 | 1.71 | 1.81 | 1.76 |
| Cr | 15.9 | 18.1 | 15.5 | 16.5 | 27.6 | 23.4 | 21.9 | 24.3 | 7.08 | 8.03 | 8.37 | 7.83 |
| La | 8.71 | 8.52 | 8.40 | 8.54 | 10.8 | 11.0 | 11.1 | 11.0 | 9.99 | 10.8 | 10.8 | 10.5 |
| Br | 35.4 | 35.4 | 34.3 | 35.0 | 32.6 | 28.5 | 30.4 | 30.5 | 19.6 | 14.9 | 15.6 | 16.7 |
| Sb | 0.84 | 0.85 | 0.87 | 0.856 | 1.03 | 0.98 | 1.06 | 1.02 | 0.40 | 0.38 | 0.31 | 0.346 |
| Cs | 4.16 | 4.13 | 4.16 | 4.15 | 4.38 | 4.20 | 4.52 | 4.37 | 2.20 | 2.12 | 1.89 | 2.07 |
| Sc | 9.19 | 9.21 | 8.92 | 9.11 | 10.1 | 10.2 | 10.4 | 10.2 | 12.7 | 12.9 | 15.4 | 13.67 |
| Rb | 19.1 | 19.5 | 17.8 | 19.0 | 26.6 | 22.6 | 25.7 | 25.0 | ND | ND | ND | ND |
| Co | 6.57 | 6.61 | 6.32 | 6.50 | 6.92 | 6.74 | 7.03 | 6.90 | 9.47 | 9.58 | 9.38 | 9.61 |
| Ta | 0.295 | 0.208 | 0.271 | 0.256 | 0.348 | 0.272 | 0.242 | 0.287 | ND | ND | ND | ND |

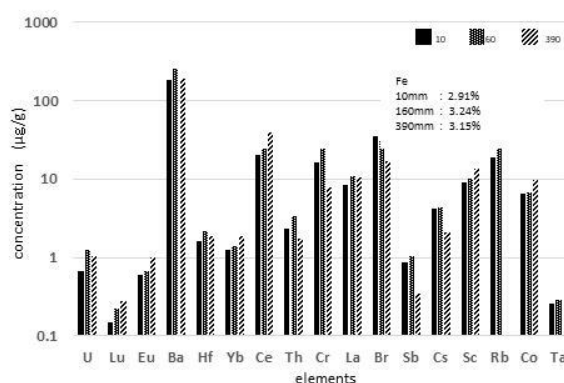


Fig. 1. Determination of trace elements in sediments of Lake Onuma on Mt. Akagi

Fe contained about 3%. Ba was at a concentration of 100 $\mu\text{g/g}$ to 200 $\mu\text{g/g}$. Also, Ce, Cr, Br and Ba are at concentration range levels of 10 $\mu\text{g/g}$ to 100 $\mu\text{g/g}$, and Hf, Yb, Th, Cs, Sc and Co are concentration range levels of 1 $\mu\text{g/g}$ to 10 $\mu\text{g/g}$.

REFERENCES:

- [1] K. Suzuki *et al.*, Science of the Total Environment, **622-623**(2018)1153-1164.
- [2] M. Mori *et al.*, Science of the Total Environment, **575**(2017)1247-1254.

N. Hasebe, K. Miura¹, M. Ogata, U. Uyangaa¹, K. Kinugawa¹, R. Januar¹, K. Oohashi², Y. Minomo², and Y. Iinuma³

Institute of Nature and Environmental Technology, Kanazawa University

¹*Graduate School of Natural Science and Technology, Kanazawa University*

²*Graduate School of Science and Technology for Innovation, Yamaguchi University*

³*Institute for Integrated Radiation and Nuclear Science, Kyoto University*

INTRODUCTION: Luminescence dating observes the natural accumulated radiation damage caused by radioisotopes such as U and Th as the form of glow after stimulation by heating or lightening. Because of age range applicable, luminescence dating has been applied to Quaternary active fault (e.g., Ganzawa et al., 2013). However, little comprehensive studies on the effect of rock deformation or destruction through the faulting on luminescence signal have been reported so far. In this study, quartz with known radiation dose is prepared and artificially ground to understand the behavior of luminescence sites during the faulting.

EXPERIMENTS: First, quartz were extracted from granitic specimen by conventional mineral separation processes. To cancel naturally accumulated doses in the environment, quartz were left under the LED light at 80°C for 12 hours. Samples were then wrapped with aluminum foil and irradiated at gamma-ray irradiation facility at KUR to give a known dose of 60 Gy. To check the initial status, some part of samples were brought to Kanazawa University and optically stimulated luminescence (OSL) was measured. Afterwards, samples were brought to Yamaguchi University and friction experiment to mimic fault activity was performed.

RESULTS: The OSL shows typical quartz signal with rapidly decreasing intensity (Fig. 1). When intensity of stimulated light is linearly increased, LM-OSL signal profile is obtained and it can be deconvoluted depending on the sensitivity in releasing light (Fig. 2). The main is the fast component. After the measurement, additional artificial dose of 5 Gy was given by built-in x-ray facility and OSL was measured again. When main 60 Gy signal is compared to the 5 Gy x-ray signal, the signal intensities were smaller than expected (Fig. 3) and showed a wide variation. The reason they show smaller values may be attributable to the unstable luminescence sites in the granitic quartz. Because luminescence signal is too small to perform friction experiment, additional irradiation experiment will be necessary to move to the next step.

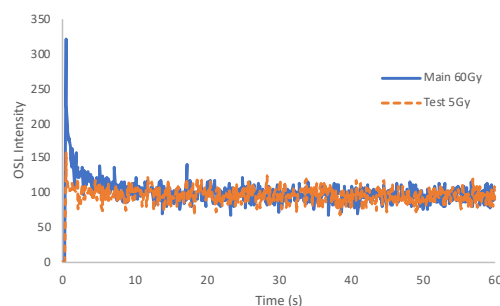


Fig. 1. Example of OSL signal after gamma irradiation (main 60 Gy) and x-ray irradiation (Test 5 Gy).

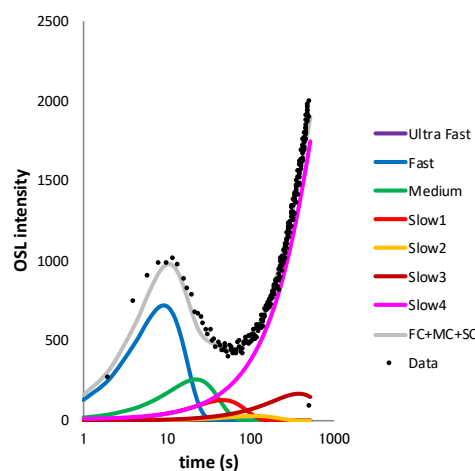


Fig. 2. Example of LM-OSL signal and the results of deconvolution.

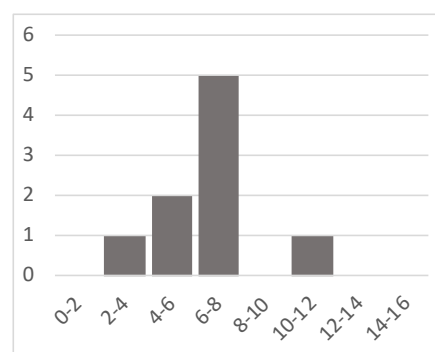


Fig. 3. Histogram for main/x-ray intensity ratio.

CO5-16 Elemental Composition of Atmospheric Fine Particulate Matter (PM_{2.5})

Y. Oura, J. Kaneko, R. Taniguchi, Md. S. Reza

Department of Chemistry, Tokyo Metropolitan University

INTRODUCTION: Although various sizes of particulate matters suspend in the atmosphere, an influence of very fine particles of less than 2.5 μm of aerodynamic radius (PM_{2.5}) on human health has been attracting attention. Organic compounds, which are considered to be harmful, in PM_{2.5}, are actively determined, but inorganic analysis such as elemental composition is also indispensable for particle characterization. We collected PM_{2.5} in Hachioji and Koto for 4 years from 2006, and their elemental compositions were determined by instrumental neutron activation analysis (INAA). Recently the environmental standards of PM_{2.5} are almost achieved every year in Tokyo. But PM_{2.5} is still a matter of concern at present. Therefore, elemental composition of the present PM_{2.5} was determined by INAA and compared with ones of PM_{2.5} collected about 10 years ago.

EXPERIMENTS: Using a NILU filter holder with successive PM₁₀ and PM_{2.5} inlets, PM_{2.5} was collected on a Nuclepore polycarbonate filter of 0.2 μm of pore size for two weekdays every week from June to December at a rooftop of a building in Minami-Osawa campus of Tokyo Metropolitan University. Mass concentration in $\mu\text{g m}^{-3}$ was determined by weighing the filter before and after collection of PM_{2.5}.

Polycarbonate filters on which PM_{2.5} had been collected were cut in half, then one half was folded in square (10 mm \times 10 mm). Quadrangular sample in clean polyethylene bag was irradiated together with reference materials (NIST 1648, NIST 1632c, NIES No.8, and GSJ JB-1a) and sulfamic acid by neutrons for 5 minutes in Pn-3 at KUR (1 MW operation) and 1 hour in Pn-2 at KUR (5 MW operation). After irradiation only filters were transferred to a new polyethylene bag and gamma-rays were measured by Ge detector.

RESULTS: Distribution of mass concentrations in 2008, 2009, and 2018 are shown as a boxplot in Fig.1. In 2008 and 2009 PM_{2.5} was collected by the same way as in 2018 but collection periods in 2008 and 2009 were different from 2018. Average of mass concentration in 2018 was about 1/2 of one in 2008 and slightly smaller than one in 2009.

Annual averages of elemental concentrations determined using radionuclides produced by the irradiation for 5 minutes are shown in Fig.2. Determined elements are arranged in order of decreasing their average in 2018. Although ²⁷Mg was also detected, its average is not

shown in Fig.1 because a contribution of the interference reaction, ²⁷Al(n, p)²⁷Mg, had not been corrected. Sulfur was most abundant among elements determined for 3 years and In was least abundant. The similar tendency of elemental abundances was observed for 2008, 2009, and 2018. Although mass concentrations in 2008 were generally higher than ones in 2009 and 2018, elemental concentrations in 2008, 2009, and 2018 were not largely different from each other. It is guessed that concentration of carbon, which is one of the major components, varies from year to year. For Al, the difference between averages in 2008 - 2009 and one of 2018 is slightly larger than other elements. In March 2008 and 2009, some Al concentrations of larger than 450 ng m^{-3} were observed due to probably yellow sand. On the contrary collection of PM_{2.5} had been started in July in 2018 and such high Al concentration was not observed. It is the main reason of the difference for Al.

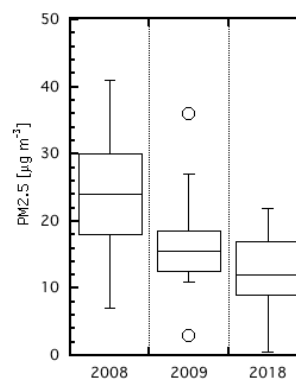


Fig. 1. Mass concentrations of PM_{2.5} in 2008, 2009, and 2018.

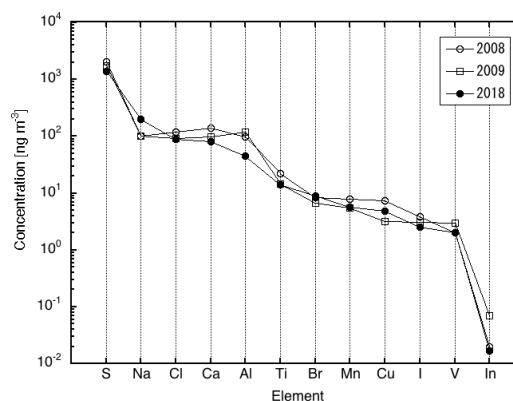


Fig. 2. Elemental concentration of PM_{2.5} in 2008, 2009, and 2018. Elements are arranged in order of decreasing their average in 2018.